JOURNAL OF MATERIALS SCIENCE 27 (1992) 3756–3762

Spherical and rod-like zinc oxide microcrystals: morphological characterization and microstructural evolution with temperature

M. ANDRÉS-VERGÉS*, M. MARTÍNEZ-GALLEGO
Departamento de Química Inorgánica, Facultad de Ciencias, Universidad de Extremadura, 06071 Badajoz, Spain

Spherical ZnO microcrystals obtained by spray pyrolysis and thermal decomposition methods as well as rod-like ZnO particles (prismatic and needle shaped) prepared from precipitation in aqueous solutions, have been characterized by electron microscopy, X-ray diffraction and infrared spectroscopy. Very different sizes of ZnO particles were obtained from spray pyrolysis. However, only the larger particles (0.7 μm) were found to be slightly deformed by infrared spectroscopy. From thermal decomposition of zinc acetate, fine particles of average size 0.05 μm, rather spherical and agglomeration free were obtained. The role of initial size and morphology in the thermal evolution is fundamental: very fine spherical particles (0.01–0.02 μm), can be sintered to give particles of 0.1–0.3 μm at 875 °C with unchanged morphology. When the temperature induces a change in spherical shape, the first microstructural changes appear to take place through the crystallographic *c*-axis. However, for rod-like particles, changes begin from the *a, b* axes, being faster for needle-shaped microcrystals.

1. Introduction

It is well known that zinc oxide presents interesting physico-chemical properties, rendering it a suitable compound for widespread applications, such as ceramic material in electro-optical devices and varistors, a semiconductor, in the rubber industry and in pharmaceutical and cosmetic products, etc.

In order to improve the properties which are dependent on the zinc oxide surface, control of morphology and particle size is required. With this aim, several authors have developed new ways for obtaining homogeneous zinc oxide microcrystals. Spherical particles have been obtained by spray pyrolysis [1] and aqueous precipitation [2] procedures, and rod-like particles have been prepared by homogeneous precipitation in an aqueous medium [3, 4], thermal decomposition of organometallic zinc complexes [5] and calcination of basic zinc carbonate powders [6] among other procedures.

In this paper, an alternative method for obtaining spherical zinc oxide powders is presented. The procedure is based on the thermal decomposition of zinc acetate (TD). In addition, an exhaustive characterization of spherical and rod-like particles is carried out. With this purpose, the thermal evolution of zinc oxide powders, prepared from different procedures and/or conditions, is followed by X-ray diffraction, electron microscopy and infrared spectroscopy.

Satisfactory interpretation of experimental infrared spectra can be carried out from the pure phonon theory known as the theory of average dielectric constant (TADC), which was generalized by Hayashi *et al.* [7] for the case of randomly oriented ellipsoidal particles having anisotropic dielectric constants.

From the TADC, the shape and agglomeration state of the powder particles can be derived, so this theory represents a powerful tool in the evaluation of modern powder preparation techniques. The infrared spectra corresponding to a large number of monodispersed small ionic crystals appear to have been successfully interpreted in recent literature [4, 8–13].

2. Experimental procedure

2.1. Materials

All chemicals were of reagent grade and the solutions were filtered through 0.22 μm pore size Millipore filters to remove any contaminant particles.

2.2. Preparation of zinc oxide powders

2.2.1. Spray pyrolysis

Two samples, SP and SP′, were obtained according to a procedure described previously [1, 8]. The particular conditions were: a methanol solution of 0.014 M zinc acetate (SP) and a methanol solution of 0.067 M zinc nitrate (SP′).

* Author to whom all correspondence should be addressed.

0022–2461

2.2.2. Thermal decomposition

Zinc acetate was calcined in a furnace at 400 °C for 4 h up to full decomposition [14].

2.2.3. Aqueous precipitation

The procedure followed to prepare the rod-like particles was described previously [4]. Representative monodispersed microcrystals were obtained under the conditions: 0.05 M zinc nitrate and 0.05 M hexamethylenetetramine for the synthesis of prismatic particles (P) (see Fig. 8a); 0.01 M zinc nitrate and 0.05 M hexamethylenetetramine for needle particles (N) (see Fig. 8b). In both cases, the solutions were maintained at 100 °C for 30 min.

The powders prepared from each procedure were heated at temperatures between 600 and 1300 °C for 6 h in an oven.

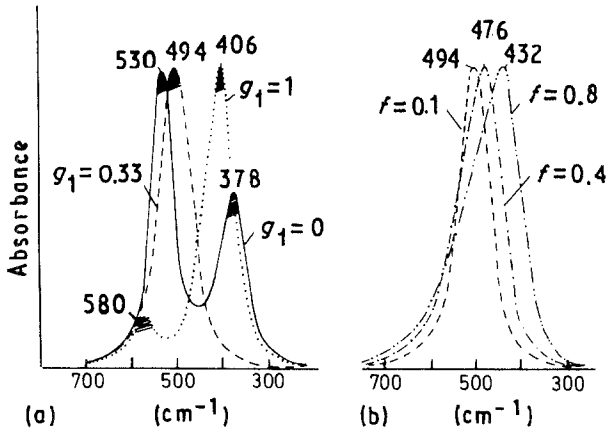

Figure 1 Calculated spectra for ZnO microcrystals (a) with different shape factors and $f = 0.1$, (b) with different filling factors and $g_1 = 0.33$. Striped ($E_{\|c}$) and solid ($E_{\perp c}$) shaded bands are originated by each polarization mode.

3. Morphological characterization

In order to study the different samples as well as their evolution with temperature, X-ray diffraction (XRD) patterns (Philips PW 1729), transmission (TEM) and scanning (SEM) electron micrographs (Philips 300 and Jeol T-100 respectively) and infrared spectra (Perkin Elmer 580B, KBr pellets) were obtained. The XRD patterns corresponding to rod-like particles were recorded as oriented aggregates.

The experimental infrared spectra were analysed by means of the TADC. A theoretical background can be found in the literature [7, 15, 16]. In this theory, the influence that the shape and agglomeration state of the particles have on the two transverse optical modes of the zinc oxide ($w_{T\|} = 377\ cm^{-1}$ and $w_{T\perp} = 406\ cm^{-1}$) is taken into account through the depolarization or shape factor, g, and filling factor, f, respectively. The particle shape is assimilated to a revolution ellipsoid through a g factor associated with the crystallographic axes of the crystal. The shape factor associated with the c-axis is called g_1; its value ranges between 0 for the cylinder and 1 for the slab, being 0.33 for the sphere and such that $g_1 + 2g_2 = 1$. The filling factor, f, represents the fraction of the total sample volume occupied by the ellipsoids, and its value ranges between 0 and 1.

In order to illustrate the influence that these factors have on the position and intensity of the two optical modes, calculated infrared spectra are represented in Fig. 1. It must be noted that the damping parameters of each vibrational mode were multiplied by factors close to 5 to approximate the experimental peak broadening.

It can be seen from Fig. 1a, that the two absorption bands of zinc oxide move in opposite directions as the particles shape varies from the slab ($g_1 = 1$) to the cylinder ($g_1 = 0$) morphology. The crossing of the absorption bands is such that for g_1 values close to the sphere they overlap, giving rise to a simple band at about $494\ cm^{-1}$. Therefore, from the spherical morphology, an increase in the splitting of the absorption bands is produced as the prolative or plate-like shape is reached.

On the other hand, if the spherical morphology remains constant and the agglomeration state is varied, the spectra show in all cases a single band which is shifted from $494\ cm^{-1}$ ($f = 0.1$) to $432\ cm^{-1}$ ($f = 0.8$). However, in general, when non-homogeneous morphologies are present in a powder, special care must be taken in the analysis of the experimental infrared spectra because several bands can overlap giving an infrared spectrum which can be the subject of misleading conclusions.

4. Results and discussion

4.1. Spray pyrolysis

Figs 2 and 3 show the electron micrographs corresponding to SP and SP′ powders as well as their evolution with temperature. The initial particles observed by SEM (Figs 2a, 3a) show a spherical morphology in both cases, with an average size of 0.2 and 0.7 μm, respectively. However, when the SP sample is observed by TEM (Fig. 2b), a non-homogeneous arrangement of smaller particles, called primary particles (0.01–0.02 μm), appears. Therefore, the larger particles (secondary particles) can be considered to be formed by agglomeration of the primary particles. Furthermore, some aspects of the SP′ sample should be noted: (i) the primary particles are very scarce, being mostly integrated inside the secondary particles (Fig. 3b); (ii) these particles appear more firmly packed than particles obtained from zinc acetate solution.

When the SP sample is heated above 600 °C, most of the primary particles disappear, and the secondary particles appear to be more closely and firmly packed. At 875 °C, only one kind of particle is observed (Fig. 2c) with a particle size between 0.1 and 0.3 μm, which can be explained through a sintering process from the primary particles. It must be noted that these internal changes are not observed by SEM; the same aspect remains throughout this temperature interval.

For the SP′ sample, the evolution with temperature is rather different; SEM at 875 °C (Fig. 3c) shows an appreciable sintering between the secondary particles, increasing the average size from 0.7 μm to 1 μm.

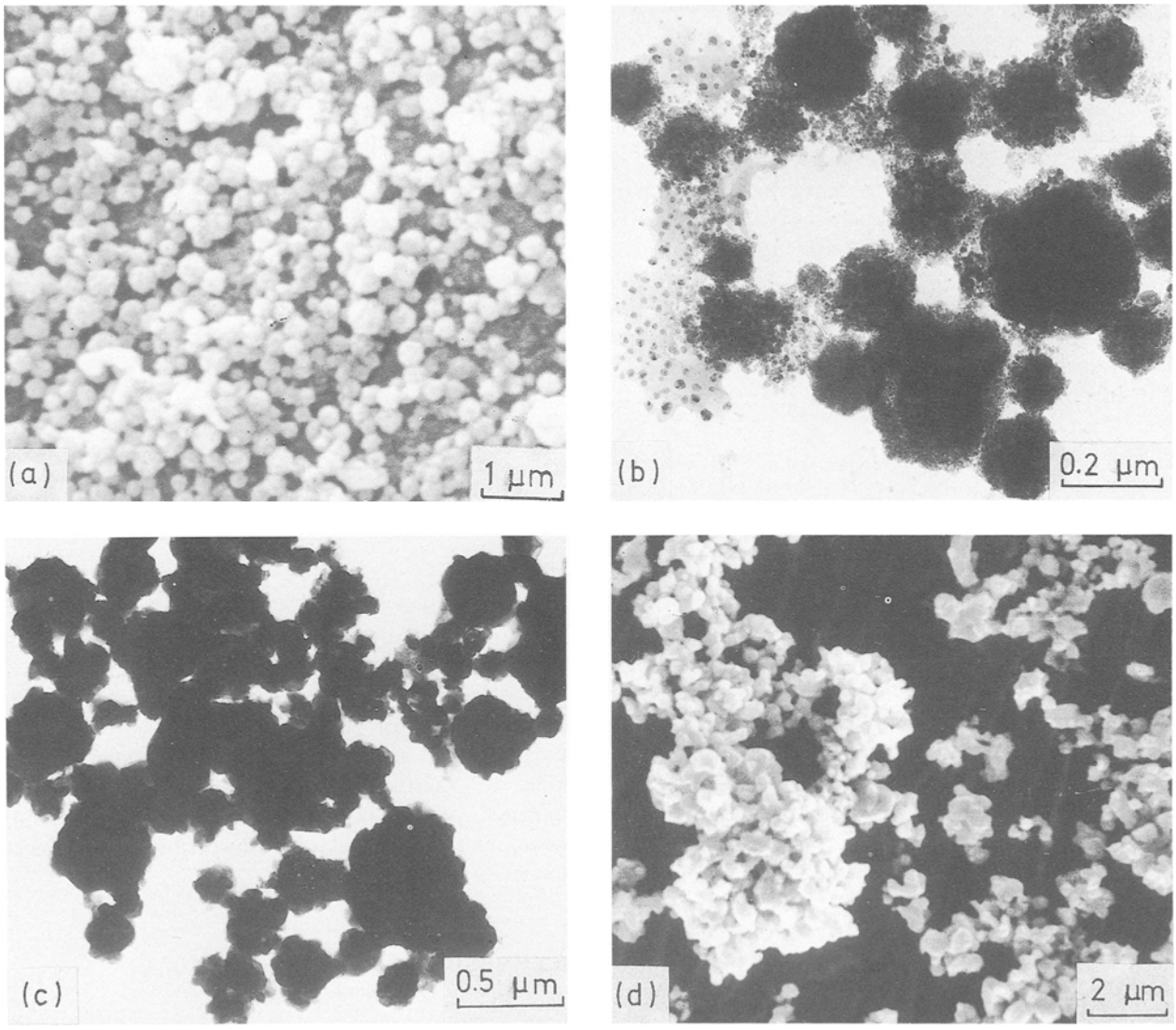

Figure 2 Electron micrographs of ZnO microcrystals obtained by spray pyrolysis. (a) SEM, and (b) TEM of the initial sample SP, (c) TEM SP-875; (d) SEM SP-1025.

XRD patterns (Fig. 4) are in agreement with the electron micrographs. Two facts must be pointed out: (i) the SP sample is less crystalline than SP′, which may be due to its smaller particle size, and (ii) the crystallinity in both samples improves as the temperature is raised as a consequence of sintering.

At higher temperatures, both sintering and agglomeration of the secondary particles take place (Figs 2d, 3d), the resulting particles ranging in size between 0.1 and 0.8 μm for SP (1025 °C), and about 1.5 μm for SP′ (1150 °C).

Further conclusions can be drawn from the analysis of the infrared spectra (Fig. 5). The differences observed in the SP and SP′ spectra can only be attributed to morphological differences because particle sizes below 10 μm do not affect the infrared spectrum [17], and the agglomeration state can shift one or more bands but cannot cause their splitting (Fig. 1b). The single band centred at 460 cm^{-1} (SP), must be assigned to spherical particles, but when band splitting occurs, prolative or platelike shapes are present (see Section 3). In SP′, the bands at 490 and 442 cm^{-1} are assigned to the $w_{T\perp}$ and $w_{T\parallel}$ modes, respectively; therefore, for SP′ it can be concluded that slightly prolate particles are obtained. An initial sintering between secondary particles may be a probable explanation for this fact. The infrared spectra at 600 and 875 °C (the shoulder is reinforced with temperature), as well as the SEM of Fig. 3c, endorse this argument.

For the same temperature interval, the SP sample shows one band shifted to different frequencies. As pointed out, this fact is successfully explained from variations in the state of agglomeration of the spherical morphology, and the spectra SP, SP-600 and SP-875 are well reproduced with filling factors 0.5, 0.8 and 0.4, respectively. These results suggest that the initial sample heated at 600 °C increases its agglomeration state from 0.5 to 0.8, which can be interpreted by TEM as being due to a sintering and growth of the primary particles. The reduction in agglomeration of the particles between 600 and 875 °C may be explained by a total sintering of the primary particles, leaving the secondary ones less agglomerated.

At higher temperatures (SP-1025), band splitting due to prolate morphology is produced as a consequence of a new sintering process between the secondary particles. Therefore, from the results obtained for SP′ and SP samples, it can be deduced that the

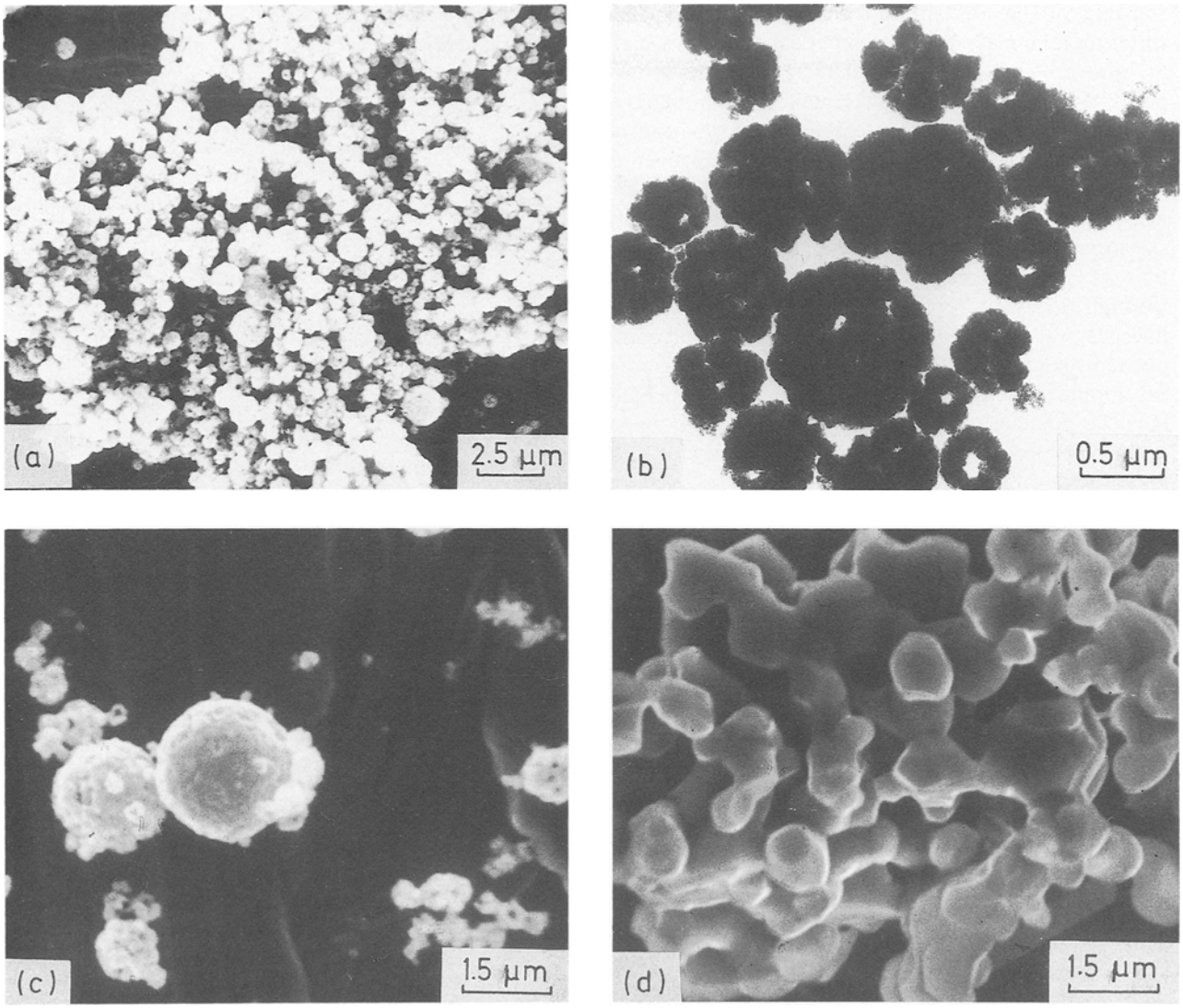

Figure 3 Electron micrographs of ZnO microcrystals obtained by spray pyrolysis. (a) SEM, and (b) TEM of the initial sample SP′, (c) SEM SP′-875, (d) SEM SP′-1150.

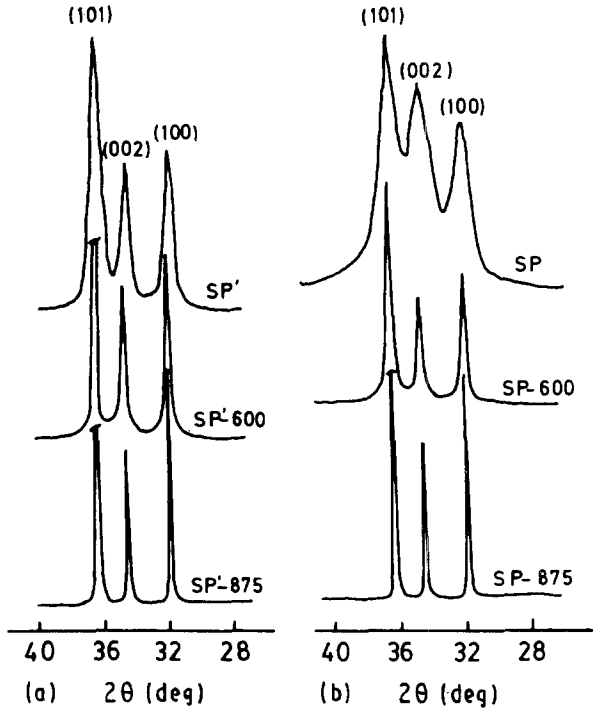

Figure 4 Evolution with temperature of the XRD patterns of ZnO microcrystals obtained by spray pyrolysis. (a) SP′ sample, (b) SP sample.

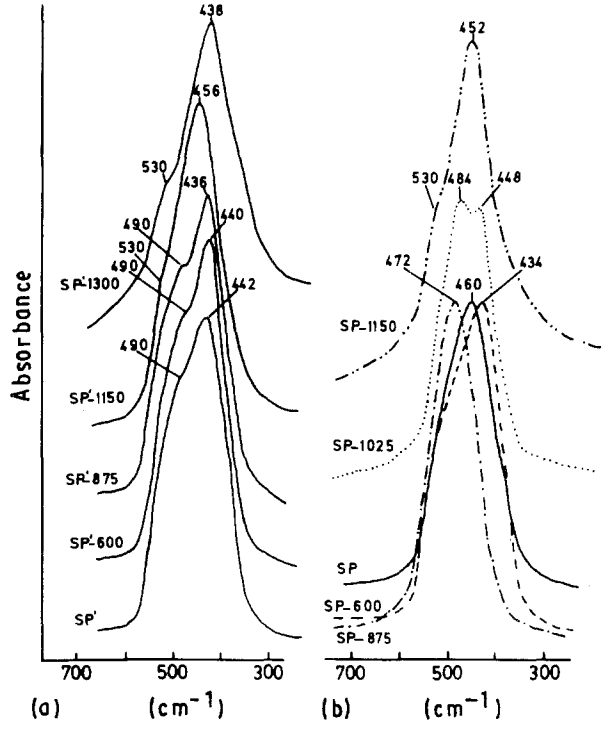

Figure 5 Evolution with temperature of the infrared spectra of ZnO microcrystals obtained by spray pyrolysis. (a) SP′ sample, (b) SP sample.

splitting of the absorption band occurs only when sintering take place between spherical particles which are above ~ 0.3 μm in size. It must be noted at this point, that the SP sample presents a thermal behaviour ($T < 1025\,^{\circ}C$) which resembles the formation of rod-like zinc oxide microcrystals in homogeneous solutions [4]. In this case, the initial crystalline spherical particles increase their size up to 0.5–1 μm. This size appears to be critical because once reached, every pair of particles begins to engage by interaction through the *c*-axes, giving rise to embryonic rod-like microcrystals which later grow from the solution complexes by some kind of ripening mechanism. When the SP sample is thermally treated, the very fine spherical particles increasing in size up to 0.1–0.3 μm by a sintering process, maintaining their spherical morphology. From this size, the sintering process takes place through the interaction of the *c*-axes, giving non-homogeneous particles, with an axial ratio $c/a > 1$.

When the temperature increases to above 1025 °C for SP and to between 875° and 1150 °C for SP′, dramatic changes are seen from the respective infrared spectra. Crossing of the bands is now produced (in SP′-1150 it is well observed) in such a manner that the shoulder at 530 cm^{-1} is due to $w_{T\|}$ mode, which is in agreement with a change in the axial ratio c/a to < 1.

4.2. Thermal decomposition

Fig. 6a shows a transmission electron micrograph of zinc oxide prepared by thermal decomposition. In this case, particles (average size 0.05 μm), with a morphology near to spherical, are obtained. As in the preceding samples, agglomeration and sintering increase with temperature, thus the particle size becomes 0.4 μm at 600 °C (Fig. 6b).

Again, a more detailed description is obtained from infrared spectroscopy. In effect, the infrared spectrum corresponding to the initial particles (Fig. 7, TD), is in agreement with a spherical morphology; the position of the maximum (480 cm^{-1}) suggests that this powder is nearly agglomeration free.

Above 600 °C, band splitting appears as consequence of the sintering between particles of 0.4 μm, as described for SP and SP′ samples.

Finally, it must be noted that morphological changes involved in the prolate–oblate transition occur at higher temperatures for this powder, which can be inferred from the comparison of the infrared spectra TD-1150 with SP-1150 and SP′-1150, respectively.

4.3. Aqueous precipitation

In Fig. 8, scanning electron micrographs corresponding to P and N particles are shown, as well as their

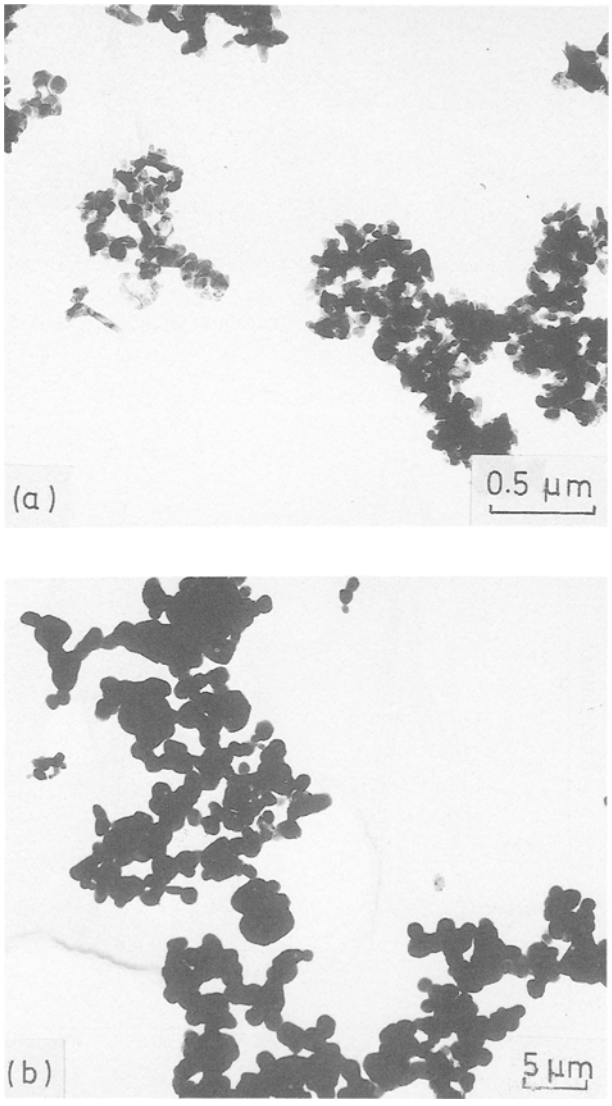

Figure 6 Transmission electron micrograph of ZnO microcrystals obtained by TD: (a) initial sample, (b) TD-600.

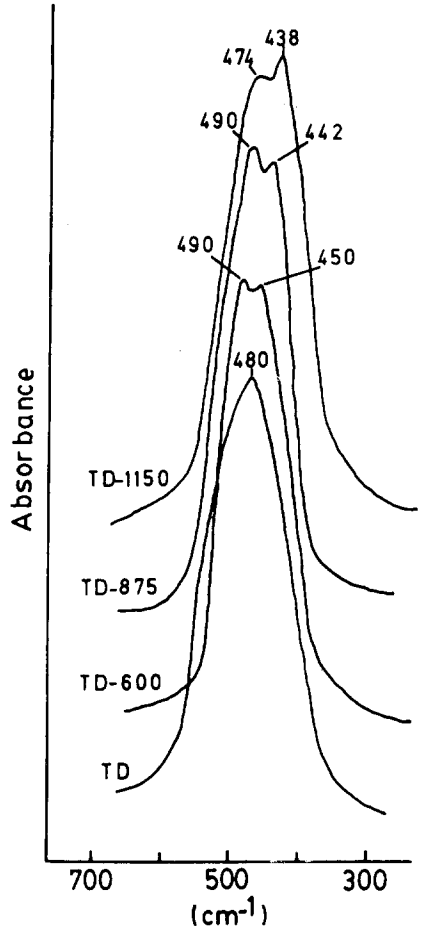

Figure 7 Evolution with temperature of the infrared spectra of ZnO microcrystals obtained by TD.

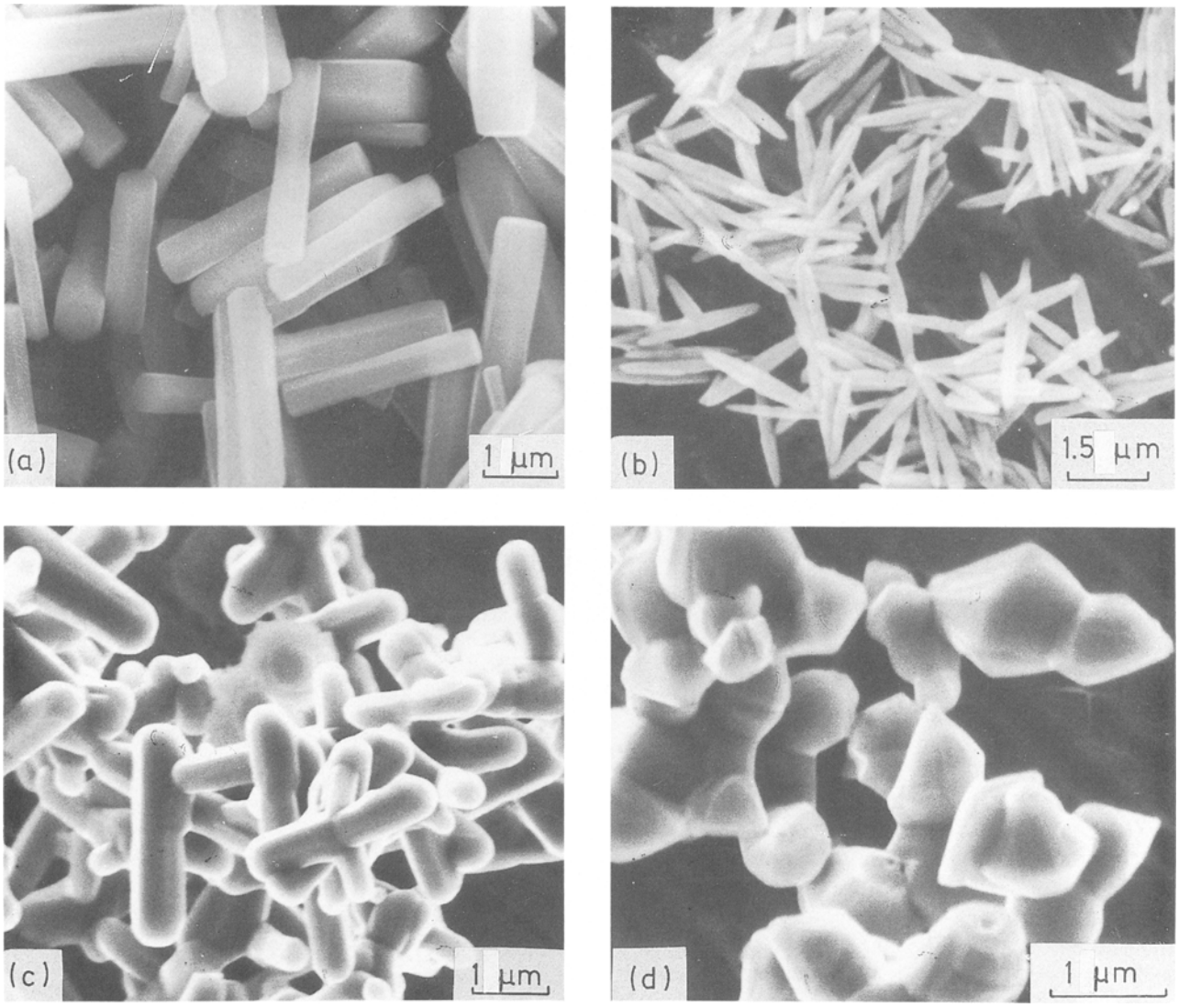

Figure 8 Scanning electron micrograph of ZnO microcrystals obtained from aqueous precipitation. (a) Prismatic shape, P; (b) Needle shape, N; (c) P-1150; (d) N-1150.

evolution at 1150 °C. Both the smaller c/a axial ratio and the greater resistance to thermal treatment for P particles than for N particles can be observed. This conclusion can also be deduced from evolution of the XRD patterns (Fig. 9). While for P particles, the relative variation in the intensities of the (0 0 2) and (1 0 0) diffraction lines is significative only at 1300 °C, for N particles, this variation is continuous from low temperatures and greater than that corresponding to P particles for the same temperature.

Similar conclusions are deduced from the infrared spectra shown in Fig. 10. The high splitting of the infrared bands observed in P and N spectra is in agreement with a fairly fibrous morphology. Nevertheless, this splitting is greater in spectrum N; so N particles will have greater c/a axial ratio values. On the other hand, the effect of temperature also can be inferred from the band splitting which decreases more quickly for N particles.

The infrared spectra obtained up to 875 °C show other interesting aspects that must be taken into account: (i) the band centred above 500 cm^{-1} is shifted while the other one remains constant, (ii) a shoulder appears at 564 and 530 cm^{-1} in P and N spectra,

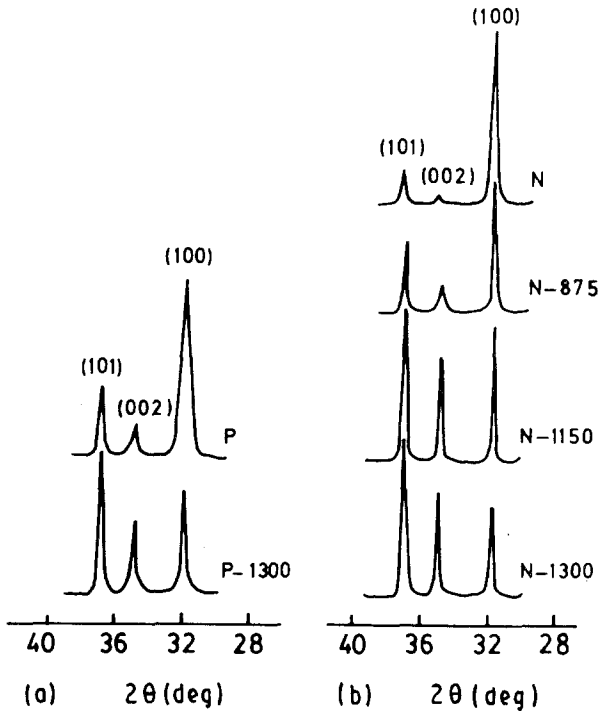

Figure 9 Evolution with temperature of the XRD patterns of ZnO microcrystals obtained from aqueous precipitation. (a) Prismatic shape, (b) needle shape.

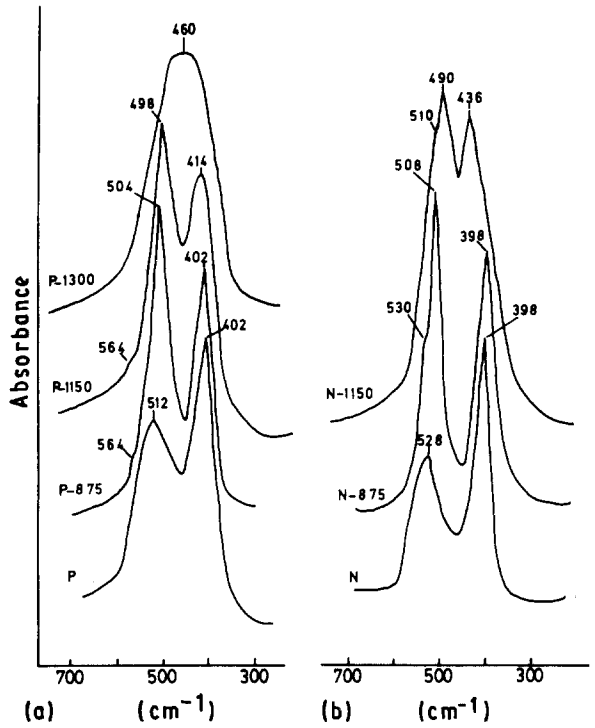

Figure 10 Evolution with temperature of the infrared spectra of ZnO microcrystals obtained from aqueous precipitation. (a) Prismatic shape, (b) needle shape.

respectively. As the band around 400 cm^{-1} is due to the $w_{T\|}$ mode, the thermal evolution of the infrared spectra in this range of temperature seems to indicate that morphological changes are developed preferentially in the *a*, *b* crystallographic directions. For the highest temperatures, the *c* axis is also affected and a marked crossing of bands is observed for P particles at 1300 °C.

5. Conclusions

1. ZnO spherical particles of very different sizes are obtained by spray pyrolysis; however, only the larger particles (0.7 μm) are shown to be slightly deformed, from the infrared spectra.

2. Thermal decomposition of zinc acetate yields fine particles of average size 0.05 μm, agglomeration free, and close to spherical morphology.

3. The aqueous precipitation method is suitable for obtaining needle-shaped and prismatic microcrystals. Both kinds of particle present a high fibrous morphology, the needle-shape having a greater *c*/*a* axial ratio.

4. On the other hand, the role of morphology in thermal behaviour is fundamental. The finer spherical powder (SP), remains unchanged until particles larger than 0.3 μm are formed above 875 °C. When the temperature alters the spherical shape, the first microstructural changes take place through the crystallographic *c*-axis. However, for rod-like particles, the changes begin from the *a*, *b* crystallographic axes and are faster for needle-shaped microcrystals. Therefore, it can be suggested that microstructural changes due to thermal treatments do not occur at random, but that they are conditioned by the crystallographic axes.

Acknowledgements

We thank Professor M. Kato for supplying the samples produced by spray pyrolysis, and Dr V. García Martínez for his assistance with the scanning electron microscopy.

References

1. T. Q. LIU, O. SAKURAI, N. MIZUTANI and M.KATO, *J. Mater Sci.* **21**(1986) 3696.
2. S. M. HAILE, D. W. JOHNSON Jr, G. H. WISEMAN and H. K. BOWEN, *J. Amer. Ceram. Soc.* **72** (1989) 2004.
3. K. FUJITA, K. MURATA, T. NAKAZAWA and I. KAYAMA, *Yogyo-Kyokai-Shi* **92** (1984) 227.
4. M. ANDRÉS-VERGÉS, A. MIFSUD and C. J. SERNA, *J. Chem. Soc. Faraday. Trans.* **86** (1990) 959.
5. E. MATIJEVIC, *Acc. Chem. Res.* **14** (1981) 22.
6. M. CASTELLANO and E. MATIJEVIC, *Chem. Marter.* **1** (1989) 78.
7. S. HAYASHI, N. NAKAMORI and H. KANAMORI, *J. Phys. Soc. Jpn* **46** (1979) 176.
8. M. ANDRÉS-VERGÉS, A. MIFSUD and C. J. SERNA, *Mater. Lett.* **8** (1989) 115.
9. J. E. IGLESIAS, J. L. RENDON and C. J. SERNA, *Appl. Spectrosc.* **36** (1982) 325.
10. C. J. SERNA, J. L. RENDON and J. E. IGLESIAS, *Spectrochim. Acta* **38A** (1982) 797.
11. M. OCAÑA, V. FORNES, J. V. GARCIA-RAMOS and C. J. SERNA, *Phys. Chem. Mineral.* **14** (1987) 527.
12. C. J. SERNA, M. OCAÑA and J. E. IGLESIAS, *J. Phys. C Solid State Phys.* **20** (1987) 473.
13. M. OCAÑA, V. FORNES, J. V. GARCIA-RAMOS and C. J. SERNA, *J. Solid State Chem.* **75** (1988) 364.
14. T. J. GARDNER, D. W. SPROSON and G. L. MESSING, Materials Research Society Symposium Proceedings, Vol 32 (Elsevier Science, 1984) p. 227.
15. L. GENZEL and T. P. MARTIN, *Phys. Status Solid* **51b** (1972) 91.
16. *Idem, Surface Sci.* **34** (1973) 33.
17. W. WADIA and L. S. BALLOMAAL, *Phys. Chem. Glasses* **9** (1968) 115.

Received 14 March
and accepted 1 July 1991